Photosynthesis Research
https://doi.org/10.1007/s11120-021-00863-x

ORIGINAL ARTICLE

An insight into spectral composition of light available for photosynthesis via remotely assessed absorption coefficient at leaf and canopy levels

Anatoly Gitelson[1] · Timothy Arkebauer[2] · Alexei Solovchenko[3,4,5] · Anthony Nguy-Robertson[1] · Yoshio Inoue[6]

Received: 26 February 2021 / Accepted: 12 July 2021

Abstract

Non-invasive comparative analysis of the spectral composition of energy absorbed by crop species at leaf and plant levels was carried out using the absorption coefficient retrieved from leaf and plant reflectance as an informative metric. In leaves of three species with contrasting leaf structures and photosynthetic pathways (maize, soybean, and rice), the blue, green, and red fractions of leaf absorption coefficients were 48, 20, and 32%, respectively. The fraction of green light in the total budget of light absorbed at the plant level was higher than at the leaf level approaching the size of the red fraction (24% green vs. 25.5% red) and surpassing it inside the canopy. The plant absorption coefficient in the far-red region (700–750 nm) was significant reaching 7–10% of the absorption coefficient in green or red regions. The spectral composition of the absorbed light in the three species was virtually the same. Fractions of light in absorbed PAR remained almost invariant during growing season over a wide range of plant chlorophyll content. Fractions of absorption coefficient in the green, red, and far-red were in accord with published results of quantum yield for CO_2 fixation on an absorbed light basis. The role of green and far-red light in photosynthesis was demonstrated in simple experiments in natural conditions. The results show the potential for using leaf and plant absorption coefficients retrieved from reflectance to quantify photosynthesis in each spectral range.

Keywords Absorbed radiation · Green light · Far-red light · Photosynthesis · Reflectance

Introduction

Green leaves of land plants absorb a substantial fraction of incident light in the green part of the spectrum (McCree 1971; Inada 1976; Gates 1980; Terashima et al. 2016). Although fractions of blue and red light in the total light absorbed by a leaf are larger than that of green light due to the presence of chlorophylls (Chl) which have absorption peaks in the blue and red regions, once absorbed by leaves, green light drives photosynthesis with a high efficiency (Inada 1976; McCree 1971; Marosvölgyi and van Gorkom 2002). The quantum efficiency of carbon fixation on an incident light basis under illumination with green light has been shown to be similar to blue light and slightly less than red. On the basis of absorbed light, the quantum yield under green light surpasses blue, but still remains smaller than red (Hogewoning et al. 2012). One reason for the lower efficiency of photosynthesis calculated on the total light absorbed at the leaf level compared to blue light is the presence of photoprotective pigments such as flavonoids and

✉ Anatoly Gitelson
agitelson2@unl.edu

✉ Alexei Solovchenko
solovchenko@mail.bio.msu.ru

1 School of Natural Resources, University of Nebraska-Lincoln, Lincoln, NE 68583, USA

2 Department of Agronomy and Horticulture, University of Nebraska-Lincoln, Lincoln, NE 68583, USA

3 Faculty of Biology, Lomonosov Moscow State University, GSP-1, Moscow, Russia 119234

4 Michurin Federal Scientific Center, Michurinsk, Russia 393760

5 Institute of Natural Sciences, Derzhavin Tambov State University, Tambov, Russia 392000

6 Graduate School of Engineering, The University of Tokyo, Tokyo 113-8656, Japan

Published online: 28 July 2021

photosynthetically uncoupled secondary carotenoids (Laisk et al. 2014).

Red and blue light are strongly attenuated in the upper layers of the leaf, whereas green and far-red light penetrate more deeply into the leaf (Cui et al. 1991; Terashima and Saeki 1985; Vogelmann 1993; Kume 2017; Terashima et al. 2016; Wolf and Blankenship 2019). It is noteworthy in this regard that the maximum rates of carbon fixation under white light are observed in the cell layers located deep in the leaf and not in the cell layers close to the leaf surface (Nishio et al. 1993) which suggests that significant light absorption occurs in the middle layers of the mesophyll (Sun et al. 1998). While blue and red light drive most of the carbon fixation that occurs in the upper cell layers of spinach leaves, green light drives CO_2 fixation deeper within leaves (Sun et al. 1998). More specifically in spinach leaves, green light-driven carbon fixation expressed on a chlorophyll content basis peaks at a depth of ca. 200 µm, whereas blue- or red light-driven carbon fixation peaks just below the epidermal cell layer (Sun et al. 1998). The same study also reported that, at depths of 200–700 µm below the adaxial surface, the green light-driven carbon fixation is 1.3- to 2-fold higher than that driven by blue or red light.

Light in the far-red region (700–750 nm) is known to accelerate photosynthesis by energizing photosystem I; there are also reports that it can also drive leaf-level photosynthesis under certain conditions (Pettai et al. 2005; Laisk et al. 2014; Zhen et al. 2019; Kono et al. 2020). This process may involve specialized far-red chlorophylls associated with photosystem II analogous to the well-known far-red chlorophylls associated with photosystem I (Pettai et al. 2005). Chlorophyll absorption in this region may also be used by plants to balance the stoichiometry of electron transport through PS II and PS I thus increasing the overall efficiency of photosynthesis since blue and green light may overstimulate PS II (Hogewoning et al. 2012; Zhen et al. 2019). However, the proportion of light in the far-red region of the spectrum in the actual budget of light captured by leaves and canopies has scarcely been investigated so far.

Summarizing the findings mentioned above, the capability of green light, and to some extent of far-red light, to drive photosynthesis is well-established at the leaf level but only for a few species. By contrast, a significant gap exists in quantification and understanding of the contribution of radiation in these spectral ranges in leaves with contrasting structures and photosynthetic pathways. To the best of our knowledge, there have been no systematic studies on this conducted at the plant level excepting a few works using modelled canopy characteristics inferred from leaf-level data (e.g., (Paradiso et al. 2011).

The primary goal of this study was to quantify absorption of radiation by leaves and plants in blue, green, red, and far-red spectral regions using absorption coefficient retrieved from leaf and plant reflectance. By this, we demonstrate the potential of reflectance as a sufficient source of information about the energy that can be potentially intercepted by plants in different parts of the spectrum and to analyze its balance at the level of plant stand or canopy in the field. Towards this end, we compared the light absorption coefficient (Gitelson et al. 2021) in three contrasting crop species (maize, soybean, and rice) at both leaf and plant levels. Then we tentatively assessed the contributions of each spectral region to the budget of light energy absorbed by leaves and plants. We sought to address the paucity of information on the potential efficiencies of radiation both in the green and far-red ranges as potential source of energy for leaf- and plant-level photosynthesis.

Conceptual framework

In Kubelka–Munk theory (Kubelka and Munk 1931), the ratio of the absorption coefficient (α) to the scattering coefficient (β), α/β, was introduced to characterize a layer of infinite thickness. This ratio (called the remission function or the Kubelka–Munk function) is a function of the infinite reflectance (ρ_{inf}) of a layer in which further increase in thickness results in non-noticeable differences in reflectance (Kortum 1969; Wendlandt and Hecht 1966):

$$f\left(\rho_{inf}\right) = \left(1-\rho_{inf}\right)^2 \Big/ 2\rho_{inf} = \alpha/\beta \quad (1)$$

Kubelka and Munk underlined that $f(\rho_{inf})$ depends exclusively on the ratio α/β "but not on the absolute numerical values of these constants" (Kubelka and Munk 1931), see also (Kortum 1969). While the remission function is based on a hypothetical optically thick layer a leaf or plant has limited optical depth and its reflectance may differ from ρ_{inf}. The relationship between the measured reflectance ρ_0 and ρ_{inf} may be retrieved from the equation (Kortum 1969):

$$f\left(\rho_{inf}\right) = \left(1 + \rho_0^2 - T_0^2\right)/2\rho_0 - 1 \quad (2)$$

where ρ_0 and T_0 are the reflectance and transmittance of a leaf or plant, respectively.

To find $f(\rho_{inf})$ the relationship ρ_{inf} vs. ρ_0 for leaves of different species in a wide range of chlorophyll content ([Chl]) was evaluated (Gitelson et al. 2003). The numerator of Eq. 2, $(1+\rho_0{}^2 - T_0{}^2)$, was close to unity (Fig. S1A) and, thus, $f(\rho_{inf}) \cong (\rho_0)^{-1}$. For leaves with ρ_0 ranging from 0 to 50% ([Chl] varying from 40 to 810 nmol/cm^2) the relationship between $f(\rho_{inf}) = \alpha/\beta$ and reciprocal reflectance, $\rho_0{}^{-1}$ was linear, with $R^2 > 0.99$ (Fig. S1B).

Plant reflectance and transmittance depend on many biochemical and structural factors (e.g. (Naus et al. 2017)) and are also affected by irradiation conditions and the geometry

(sun–viewer–object) of the measurement. Therefore, it is practically impossible to collect all the data required, especially plant transmittance, as different hybrids and cultivars or even different plants of the same species often have vastly differing canopy structures that change during the growing season. At the plant level such measurements were carried out with upward- and downward-looking radiometers affixed with cosine diffusers and positioned at ground level and above the canopy, although they may not be reliably obtained at low to moderate vegetation fractions (Hanan et al. 2002). Thus, to find the relationship between α/β and plant reflectance ρ_0 the results of transmittance and reflectance measurements of maize and soybean plants with vegetation fractions above 70% were used (Viña 2004). As at the leaf level, at plant level the relationship between $f(\rho_{inf})$ and reciprocal reflectance, ${\rho_0}^{-1}$ was linear, with $R^2 > 0.99$ (Fig. S2).

The close linear relationships between the Kubelka–Munk remission function and reciprocal reflectance found at both leaf and plant scales (Figs. S1 and S2) laid a solid foundation for the retrieval of the canopy absorption coefficient from reflectance spectra in the form:

$$\left(\rho_\lambda\right)^{-1} = \left(\alpha_{\text{pigm}} + \alpha_0\right)/\beta \tag{3}$$

where $(\rho_\lambda)^{-1}$ is the plant reciprocal reflectance, α_{pigm} is the absorption coefficient of the photosynthetic pigments, α_0 is the absorption coefficient of non-photosynthetic pigments, and β is the scattering coefficient. The leaf absorption coefficient is governed mainly by pigment content and composition and the scattering coefficient by leaf structure and thickness. The plant absorption coefficient depends on leaf biochemistry, leaf area index (LAI) and canopy architecture—leaf angle distribution (LAD). The scattering coefficient of plant is a function of plant structural properties as plant density, LAD as well as leaf structure.

A characteristic feature of the plant $(\rho_\lambda)^{-1}$ spectrum is positive values in the near infrared (NIR) region, beyond 760 nm, where neither Chl *a* nor *b* absorb light (Gitelson et al. 2003). The absorption of healthy leaves in the NIR region is negligible (Merzlyak et al. 2002), while that of plants is sizeable due to either apparent absorption (i.e., fraction of light transmitted through the canopy) and/or due to the presence of other absorbers such as 'brown' pigments produced upon the oxidation of polyphenols during leaf damage or senescence (Merzlyak et al. 2004). Thus, the plant absorption coefficient estimated via $(\rho_\lambda)^{-1}$ (Eq. 3) may be biased when α_{pigm} is comparable to α_0, specifically in the green and red edge, and at the beginning and at the end of the growing season when total absorption is small-to-moderate. Subtraction of reciprocal reflectance in the NIR, ${\rho_{\text{NIR}}}^{-1}$, eliminates or at least significantly decreases a_0 in the numerator of Eq. 3:

$$\left(\rho_\lambda^{-1} - \rho_{\text{NIR}}^{-1}\right) = \alpha_{\text{pigm}}(\lambda)/\beta \tag{4}$$

The absorption coefficient, α_{pigm}, retrieved from Eq. 4, for leaves and plants having the same pigment content but different densities (e.g., leaf structure, thickness, LAI, biomass) may be biased due to different values of the scattering coefficient, β, in the denominator of Eq. 4. For example, a crop in the vegetative stage may have the same total pigment content as in the reproductive stage but different LAI and foliar pigment content (i.e., higher foliar pigment content and smaller LAI in vegetative stage and vice versa in reproductive stage). As a result, for the same plant pigment content, in accord with Eq. 4, the retrieved α_{pigm} would be larger in the vegetative stage (due to smaller LAI and thus plant scattering coefficient β) than in the reproductive stage. This effect may be reduced, if not eliminated, using reflectance that roughly represents a plant scattering coefficient but is not affected by pigment absorption. Reflectance in the NIR region, where chlorophylls do not absorb, is closely related with plant structural properties (e.g., LAI—Fig. S3). Higher NIR reflectance in soybean than in maize is due to the difference in canopy architecture of these crops (i.e., planophile vs. spherical leaf angle distributions). Thus, to decrease the effect of differential scattering in plants with the same [Chl] and isolate α_{pigm}, ρ_{NIR} is introduced in Eq. 4:

$$\alpha_{\text{pigm}}(\lambda) \approx \left[\left(\rho_\lambda\right)^{-1} - \left(\rho_{\text{NIR}}\right)^{-1}\right] \times \rho_{\text{NIR}} = \rho_{NIR}/\rho_\lambda - 1 \tag{5}$$

The model-derived absorption coefficient allows for the derivation of absorption coefficient spectra across the photosynthetically active radiation and the far-red spectral regions, as well as accurate estimation of plant chlorophyll content in three crops with contrasting leaf structures, canopy architectures and photosynthetic pathways: maize, soybean, and rice (Gitelson et al. 2019). This model also was used for the remote estimation of plant physiological and phenological status, and the plant-level primary productivity (Peng et al. 2011; Viña et al. 2011; Gitelson et al. 2021).

Materials and methods

The study used multiple datasets of the three crop species evaluated (i.e., maize, soybean and rice) acquired for different studies (Ciganda et al. 2009; Gitelson et al. 2005, 2006, 2008, 2016, 2018, 2019; Inoue et al. 2016; Peng et al. 2017; Viña et al. 2011) in separate sites, across different years and at scales ranging from individual leaves to entire plants. The following paragraphs summarize the procedures employed. For more details on the different data collection procedures, the reader should consult the cited papers.

Study sites

Maize and soybean data collection campaigns were carried out during the growing seasons (from May to September) of 2001–2005 in three AmeriFlux sites (US-Ne1, US-Ne2, and US-Ne3), located near Mead, Nebraska, USA. Sites 1 and 2 were equipped with a center-pivot irrigation system; site 1 was under maize continuously, while site 2 was under a maize-soybean rotation (with maize in odd and soybean in even years). Site 3 was also under a maize-soybean rotation but relied entirely on rainfall (Verma et al. 2005). Maize canopy-level transmittance was measured in 2010 at the same three AmeriFlux sites. Maize and soybean canopy-level transmittances were also measured in test fields located on East Campus, University of Nebraska-Lincoln, Lincoln, Nebraska, USA.

Rice data collection campaigns were carried out during the growing season of 2009 in ten experimental plots in Tsukuba, Japan. To induce a wide range of canopy responses, four different nitrogen levels (2, 6, 14, and 16 g m^{-2}) were applied (Inoue et al. 2016).

Reflectance and transmittance at plant scale

In maize and soybean fields, canopy reflectance was measured using two inter-calibrated radiometers (USB2000, Ocean Optics, Dunedin, FL)—Table 1. One radiometer was equipped with a 25° field-of-view optical fiber pointing downward to measure upwelling radiance within a 2.4 m^2 sampling area by placing the fiber at a height of approximately 5.5 m above the top of the plants. The other sensor was equipped with an optical fiber and a cosine diffuser pointing upward to measure downwelling irradiance. Percent plant reflectance was calculated as the ratio of upwelling radiance to downwelling irradiance (Viña et al. 2011; Rundquist et al. 2004). Plant reflectance for each date was calculated as the median value of 36 reflectance measurements collected along access roads into each of the fields.

In the rice fields, reflectance measurements were taken using a portable spectroradiometer (ASD FieldSpec-Pro, Analytical Spectral Devices, Inc., Longmont, CO) with a 25° field-of-view at a nadir-looking angle from 2 m above the plants (Table 1). Percent plant reflectance was calculated as the ratio of the upwelling radiance to that of a Spectralon-Labsphere white reference (Inoue et al. 2016). More than 30 spectra were averaged for each plot to derive the representative reflectance spectrum.

Absorption coefficient in the PAR region was calculated as $\alpha_{par} = [\rho_{NIR}/\rho_{par}] - 1$, where ρ_{NIR} is the average of reflectance values in the NIR spectral region (780–900 nm), while ρ_{par} is the average of reflectance values in the PAR spectral region (400–700 nm). Absorption coefficients in the blue, green, red, and far-red regions were calculated as $\alpha_{blue} = [\rho_{NIR}/\rho_{400–500}] - 1$, $\alpha_{green} = [\rho_{NIR}/\rho_{500–600}] - 1$, $\alpha_{red} = [\rho_{NIR}/\rho_{600–700}] - 1$, $\alpha_{far\text{-}red} = [\rho_{NIR}/\rho_{700–750}] - 1$, where $\rho_{400–500}$, $\rho_{500–600}$, $\rho_{600–700}$, and $\rho_{700–750}$ are average of reflectance values in blue, green, red, and far-red regions, respectively.

Canopy transmittance (14 field campaigns in July and September 2010) was collected using two inter-calibrated radiometers (USB2000, Ocean Optics, Dunedin, FL) as used for reflectance measurements. Each radiometer was equipped with an optical fiber and a cosine diffuser pointing upward; one of them measured downwelling incident irradiance and another downwelling irradiance inside the canopies. Downwelling irradiance inside the maize canopies was measured at the level of one leaf above the ear leaf (about 1.2–1.5 m below the top of the canopy), ear leaf level, and first, second, third and sixth leaves below ear leaf. Maize plant heights ranged from 2.5 to 3.0 m and the row spacing was 0.69–0.79 m. Downwelling irradiance inside the soybean canopies was measured at half plant height and the whole plant canopy just above the soil surface place in the middle of the rows. Soybean heights ranged from 0.71 to 1.12 m and row spacing was 0.66–0.89 m. Canopy transmittance was calculated as a ratio of downwelling irradiance inside the canopy to incident downwelling irradiance.

Green leaf area index (LAI)

Green LAI of maize and soybean plants was determined destructively from samples collected in six small plots

Table 1 Summary of experimental data sets

Crops	Year	Plots	Sensor, spectral range, nm	Distance, FOV	Leaf [Chl]	LAI	Plant type
Rice (*Oryza sativa* L. japonica variety)	2009	64	ASD 350–2500	2 m, 25°	Analytical	Destructive	Erectophile, narrow leaves
Maize (*Zea mays* L.)	2003–2005	118	USB2000 400–900	5.5 m, 25°	Non-destructive and analytical	Destructive	Plagiophile, long broad leaves
Soybean (*Glycine max* (L.) Merr.)	2002, 2004	73	USB2000 400–900	5.5 m, 25°	Non-destructive and analytical	Destructive	Planophile, round leaves

(20 m × 20 m) established within each sampling site, representing major soil and crop production zones within each site (Verma et al. 2005). In the laboratory, green leaf samples were run through an area meter (LI-3100, Li-Cor, Inc., Lincoln NE) to calculate leaf area per plant. This area was then multiplied by the plant population (assessed in each plot) to obtain green LAI for each of the six plots, which were then averaged to obtain a site-level green LAI value (Viña et al. 2011).

In the rice fields, five hills per plot were sampled randomly for destructive measurements and analysis in the lab. Green LAI was determined using an area meter (LI-3100, Li-Cor, Inc., Lincoln NE) after carefully removing all senescent leaf parts (Inoue et al. 2016).

Green LAI values in three crops are presented in Table 2.

Leaf and plant chlorophyll content

The Chl content ([Chl]) of maize and soybean leaves (ear leaf in maize plants and the top-most fully expanded leaf in soybean plants) was measured in the laboratory, concurrently with spectral reflectance measurements of the same leaves using an Ocean Optics radiometer equipped with a leaf clip (Ciganda et al. 2009). Foliar reflectance measurements were used to calculate the red edge chlorophyll index (Gitelson et al. 2003):

$$\mathrm{CI}_{\text{red edge}} = \left[\left(\rho_{\mathrm{NIR}}/\rho_{720-730}\right)-1\right]$$

where ρ_{NIR} is reflectance in the NIR range 780–800 nm and $\rho_{720-730}$ is reflectance in the red edge range 720–730 nm. $\mathrm{CI}_{\text{red edge}}$ was linearly related with the destructive lab measurements of leaf [Chl]. The relationship [Chl] vs. $\mathrm{CI}_{\text{red edge}}$, calibrated on a per-year basis, was then used to retrieve leaf [Chl] (Ciganda et al. 2009; Gitelson et al. 2005, 2006). Plant [Chl] was then calculated as a product of leaf [Chl] and green LAI.

In rice, five hills per plot were randomly sampled for obtaining a measure of leaf [Chl] using a chemical analysis in the laboratory. Canopy [Chl] was then obtained by multiplying leaf [Chl] by the biomass of green leaves per m^2 of ground area (Inoue et al. 2016).

Leaf and canopy chlorophyll contents are presented in Table 2.

Results and discussion

Leaf-level analysis

Absorption coefficient spectra taken in a wide range of pigment content (Table 2) display distinct spectral features of green plants—maxima in the blue (400–500 nm) and the red (around 670 nm) as well as minimal values in the green (around 550 nm; Fig. 1a). In green leaves (the top spectra), the ratio of the absorption coefficient at 550 nm to that at 670 nm $\alpha_{550}/\alpha_{670}$ approaches 0.3 which is a more than fourfold larger than the green/red or the green/blue ratios of the leaf specific absorption coefficient of chlorophyll determined by experimental data and used in radiative transfer models (Féret et al. 2017). This also demonstrates a 20-fold larger chlorophyll absorption by leaves in the green region as compared to that in vitro, where it does not exceed 0.01–0.015 (Lichtenthaler 1983). Therefore, leaf α_λ exhibits an important source of variability that cannot be described by variation in the chlorophyll specific absorption coefficient assumed to be invariable from one species to another (Feret et al. 2008) or the spectroscopy of this pigment in vitro. Also notable is the quite high-absorption coefficient in the far-red region. In the wavelength range 705–720 nm, the ratio $\alpha_{\text{far-red}}/\alpha_{\text{red}}$ reaches 0.3 decreasing toward longer wavelengths.

Absorption coefficients increased along with an increase in leaf Chl]—Fig. 2. In leaves of all species studied, the blue fraction of the absorption coefficient was the highest followed by the red fraction and the green fraction with a pronounced drop in $\alpha_{\Delta\lambda}$ sensitivity to [Chl] > 500 mg m^{-2} especially in the blue and the red regions.

The fraction of the absorption coefficient expressed on a [Chl] basis, $\alpha_{\Delta\lambda}$/[Chl], represents an efficiency of the pigment in capturing light in the corresponding spectral range (Gitelson et al. 2016). The values of $\alpha_{\Delta\lambda}$/[Chl] dropped along with an increase in [Chl] regardless of the spectral range $\Delta\lambda$ under consideration (Fig. 3). In leaves with [Chl] above

Table 2 Minimum (Min), maximum (Max), mean (Mn), and median (Md) leaf total ($a+b$) chlorophyll content (in mg m^{-2}) and canopy chlorophyll content (in g m^{-2}), and green leaf area index (in m^2 m^{-2}) in the maize ($N=124$), soybean ($N=73$), and rice ($N=64$) sites sampled

	Maize				Soybean				Rice			
	Min	Max	Mn	Md	Min	Max	Mn	Md	Min	Max	Mn	Md
Leaf [Chl]	231	800	567	581	80	623	358	362	152	584	322	294
Canopy [Chl]	0.07	3.61	2.04	2.13	0.03	2.69	1.07	0.97	0.01	2.13	0.63	0.53
$\mathrm{LAI}_{\text{green}}$	0.17	5.52	3.49	4.04	0.16	5.45	2.59	2.62	0.08	6.73	2.13	2.14

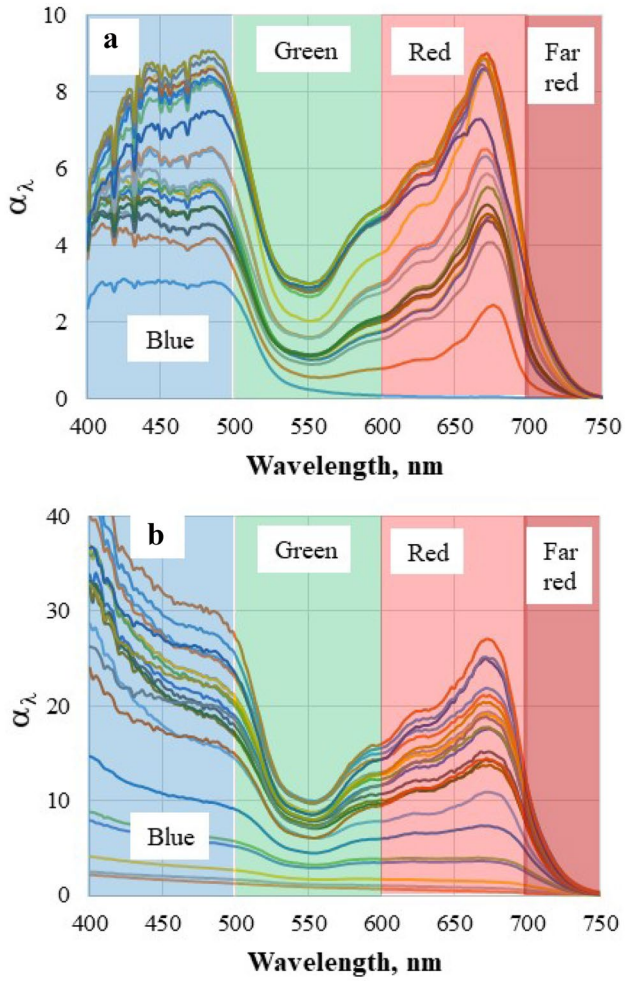

Fig. 1 Absorption coefficient spectra of maize leaves (**a**) and canopies (**b**). Absorption coefficient at wavelength λ was calculated as $\alpha = (\rho_{NIR}/\rho_\lambda - 1)$ where ρ_{NIR} and ρ_λ are reflectances of leaf and plant in the NIR and at wavelength λ, respectively. Leaf color changes from yellow (bottom spectrum) to dark green (top spectra). Canopy absorption coefficient was retrieved from canopy reflectance spectra measured across the growing season. Bottom spectra represent the beginning of the vegetative stage with low vegetation cover and senescence at the end of the season. The top spectra correspond to maximal crop green leaf area

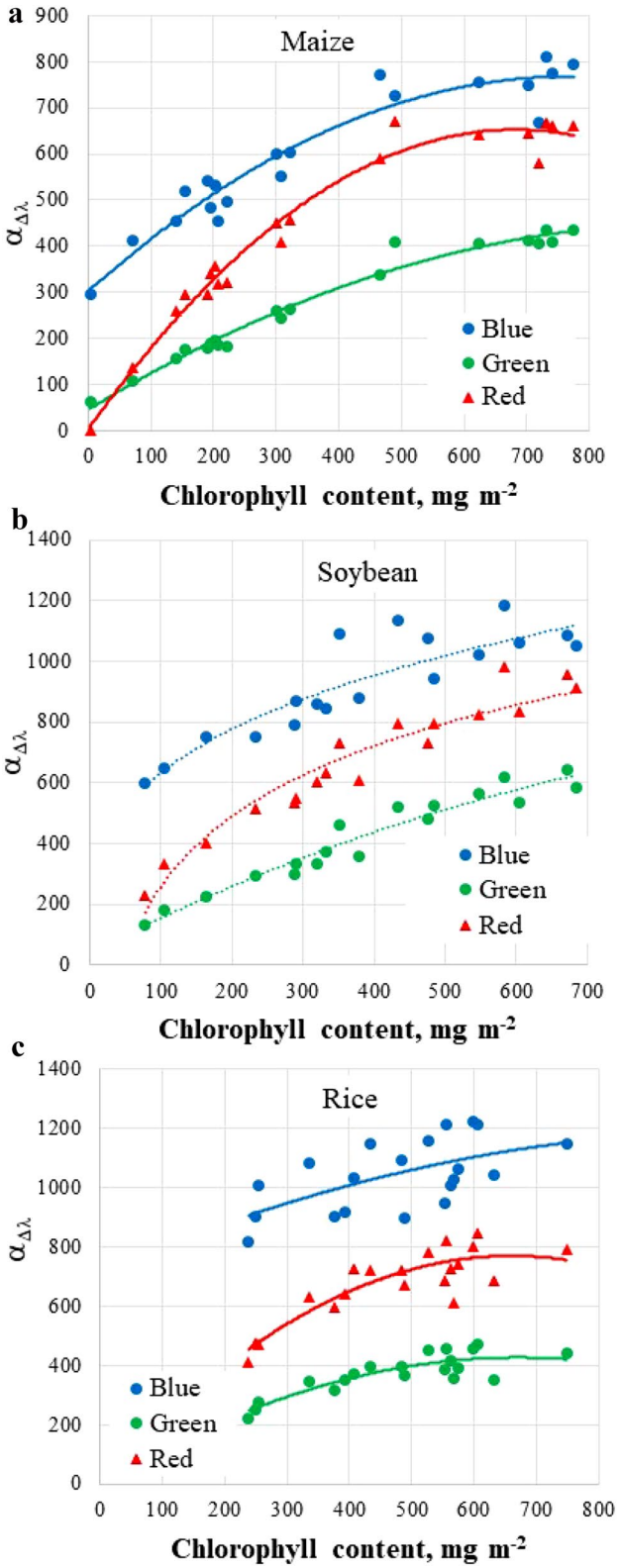

Fig. 2 Leaf absorption coefficient $\alpha_{\Delta\lambda}$ in blue, green, and red spectral ranges plotted versus leaf chlorophyll content in **a** maize, **b** soybean, and **c** rice. $\alpha_{\Delta\lambda}$ were calculated as $\alpha_{blue} = [\rho_{NIR}/\rho_{400-500}] - 1$, $\alpha_{green} = [\rho_{NIR}/\rho_{500-600}] - 1$, and $\alpha_{red} = [\rho_{NIR}/\rho_{600-700}] - 1$, where $\rho_{400-500}$, $\rho_{500-600}$, $\rho_{600-700}$ are average of leaf reflectance values in blue, green, and red regions, respectively

500 mg m^{-2} Chl efficiency decreased threefold in the blue range, twofold in red, and 1.6-fold in green.

Relationships of fractions of absorption coefficient in spectral regions $\Delta\lambda$, $\alpha_{\Delta\lambda}/\alpha_{par}$ versus leaf [Chl] (Fig. 4) bring information about the contribution of radiation absorbed in each spectral region to the total absorption by leaf in the PAR region (400–700 nm). In each spectral region the differences in the $\alpha_{\Delta\lambda}/\alpha_{par}$ vs. [Chl] relationships between the three species were very small (Fig. 4).

The absorption coefficient in the far-red region (700–750 nm) was closely related to leaf [Chl] (Fig. 5). $\alpha_{far\text{-}red}$ values were close in maize and soybean and smaller

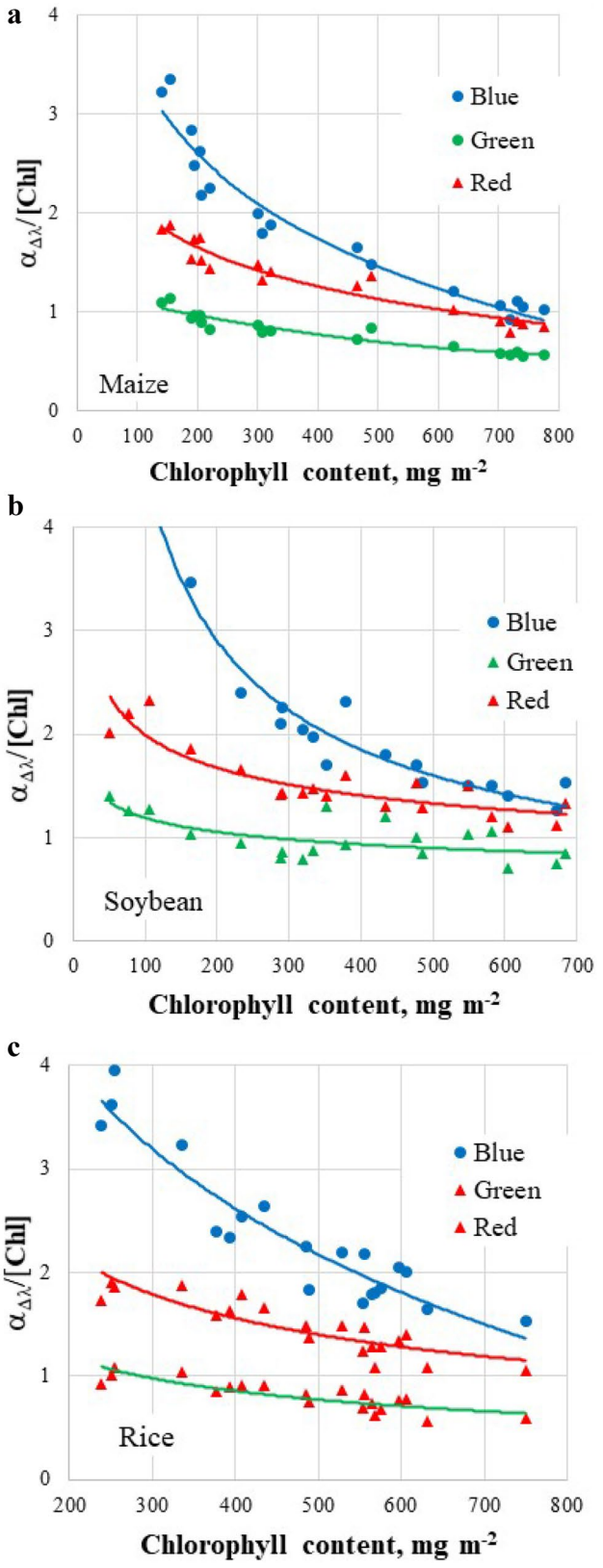

Fig. 3 Leaf absorption coefficient $\alpha_{\Delta\lambda}$ in blue, green, and red spectral ranges calculated on [Chl] basis vs. canopy Chl content in **a** maize, **b** soybean, and **c** rice

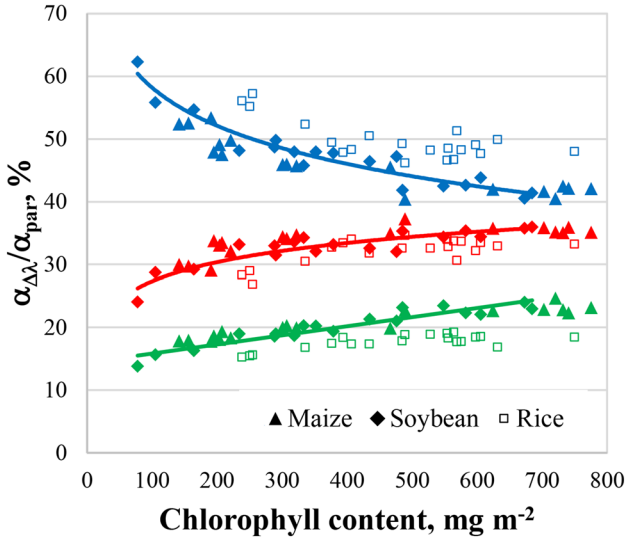

Fig. 4 Fraction of blue, green, and red light ($\alpha_{\Delta\lambda}$) in total PAR absorption by the leaf (α_{par}) plotted vs. leaf [Chl] in maize, soybean, and rice

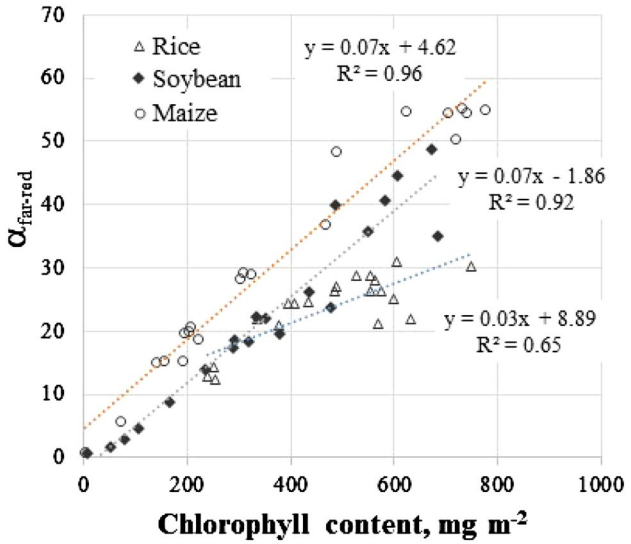

Fig. 5 Absorption coefficient in the far-red region $\alpha_{far\text{-}red}$ plotted versus leaf chlorophyll content in maize, soybean, and rice. $\alpha_{far\text{-}red}$ was calculated as $\alpha_{far\text{-}red} = [\rho_{NIR}/\rho_{700-750}] - 1$, where $\rho_{700-750}$ is average of leaf reflectance values in far-red region

in rice. The far-red fraction, $\alpha_{far\text{-}red}/\alpha_{par}$, at maximal [Chl] values was highest in maize (3%) followed by soybean (2%) and smallest in rice (1.5%). The ratio $\alpha_{far\text{-}red}/\alpha_{red}$ varied from 10% in maize, 6% in soybean and to 5% in rice.

Plant-level analysis

Spectra of the absorption coefficient at the plant level retrieved from maize reflectance measured throughout a growing season (Fig. 1b) illustrate the main features of absorption by chlorophylls (in the red) and the combined absorption of carotenoids, phenolic compounds, and chlorophylls (in the blue). Notably, the ratios $\alpha_{\text{far-red}}/\alpha_{\text{par}}$ and $\alpha_{\text{green}}/\alpha_{\text{par}}$ were at least 25% higher than at the leaf level (Fig. 1a) illustrating an increasing contribution of green and far-red light to total absorption at the plant level. The α values in the blue-violet region of the spectrum recorded at a plant level were higher than those recorded at a leaf level (cf. Fig. 1a and b). This effect can be explained by the backscattering of light by cuticle and other superficial structures of the leaves increasing individual leaf reflectance and decreasing absorption towards shorter wavelengths.

All studied species displayed linear $\alpha_{\Delta\lambda}$ vs. [Chl] relationships (Fig. 6), which were stronger than in the leaves (Fig. 2). The sensitivity of the plant absorption coefficient to [Chl] remained almost invariable over a wide range of [Chl] from the early vegetative phase to senescence comprising a distinct feature of the absorption documented at leaf and plant levels. These results support the results of modeling carried out by Paradiso et al. (2011) showing that spectral variations of photosynthesis at the plant level are smaller than those at the leaf level.

The relationships $\alpha_{\Delta\lambda}/\alpha_{\text{par}}$ vs. plant [Chl] for each fraction of the PAR absorption coefficient in all three crops were quite similar (Fig. 7). Comparable sizes of the green and red fractions as well as their considerably more stable behavior throughout the vegetation season are the specific features observed at the plant level but not at the leaf level. Notably, the green fractions averaged over the season were 1.5–2.5% higher than the red fractions (Table 3). However, for moderate-to-high [Chl], the red fractions were higher than the green fractions.

To understand how the environment inside a canopy affects the spectral composition of the absorbed light (in terms of the red, green, and blue fractions of the absorption coefficient), we measured spectra of maize and soybean canopy transmittance. For maize canopies, the spectra were measured just above the ear leaf and at several heights below it (Fig. 8a). With an increasing number of leaf layers above the sensor, transmittance decreased and, notably the magnitude of the peak in the green region decreased about twofold from the ear leaf to the sixth leaf below the ear leaf. At the height of the ear leaf the ratio $\alpha_{\Delta\lambda}/\alpha_{\text{par}}$, averaged across the season, was comprised of 49% blue, 26% green, and 25% red (Fig. 9a). At moderate-to-high [Chl] > 1 g m^{-2}, the $\alpha_{\Delta\lambda}/\alpha_{\text{par}}$ in the red was higher than in the green (Table 3, Fig. 9a). The far-red fraction inside the canopy significantly increased reaching 3.6% of α_{par} and exceeding 10% of α_{red} (not shown).

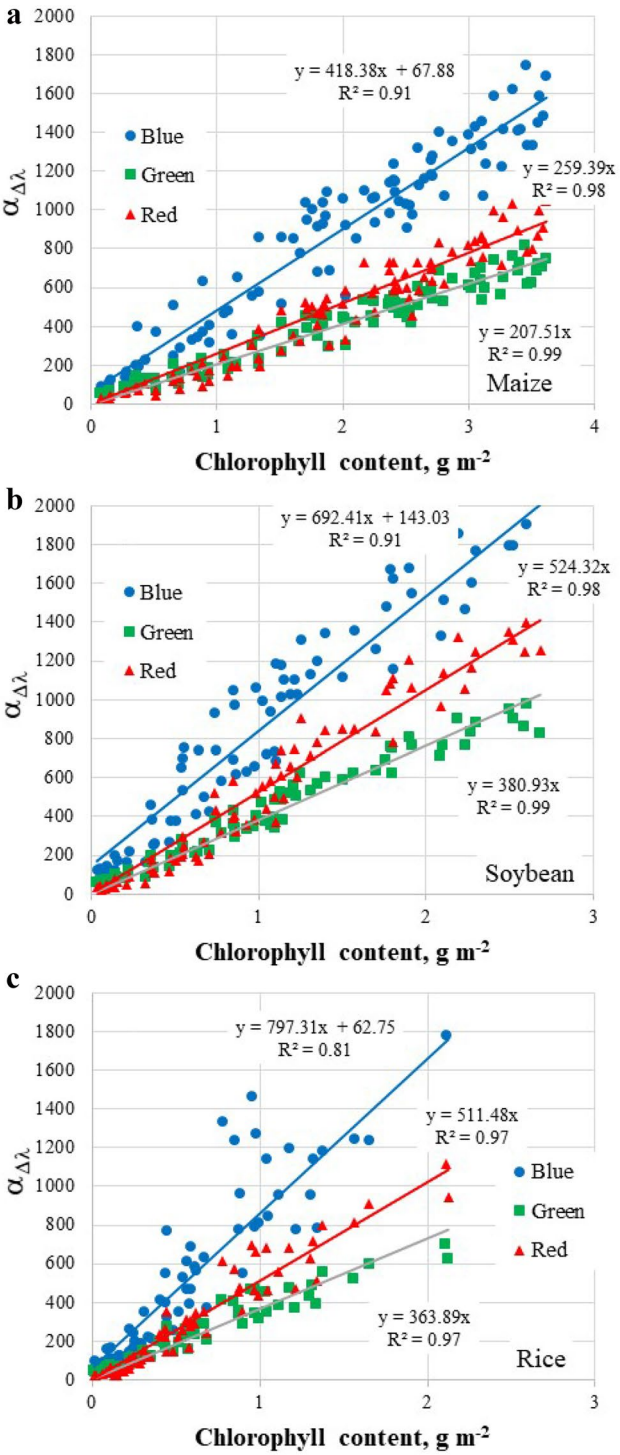

Fig. 6 Canopy absorption coefficient $\alpha_{\Delta\lambda}$ in blue, green and red spectral regions plotted versus canopy chlorophyll content in maize (**a**), soybean (**b**), and rice (**c**). $\alpha_{\Delta\lambda}$ was calculated as $\alpha_{\text{blue}} = [\rho_{\text{NIR}}/\rho_{400-500}] - 1$, $\alpha_{\text{green}} = [\rho_{\text{NIR}}/\rho_{500-600}] - 1$, and $\alpha_{\text{red}} = [\rho_{\text{NIR}}/\rho_{600-700}] - 1$, where $\rho_{400-500}$, $\rho_{500-600}$, $\rho_{600-700}$ are average of canopy reflectance values in blue, green, and red regions, respectively

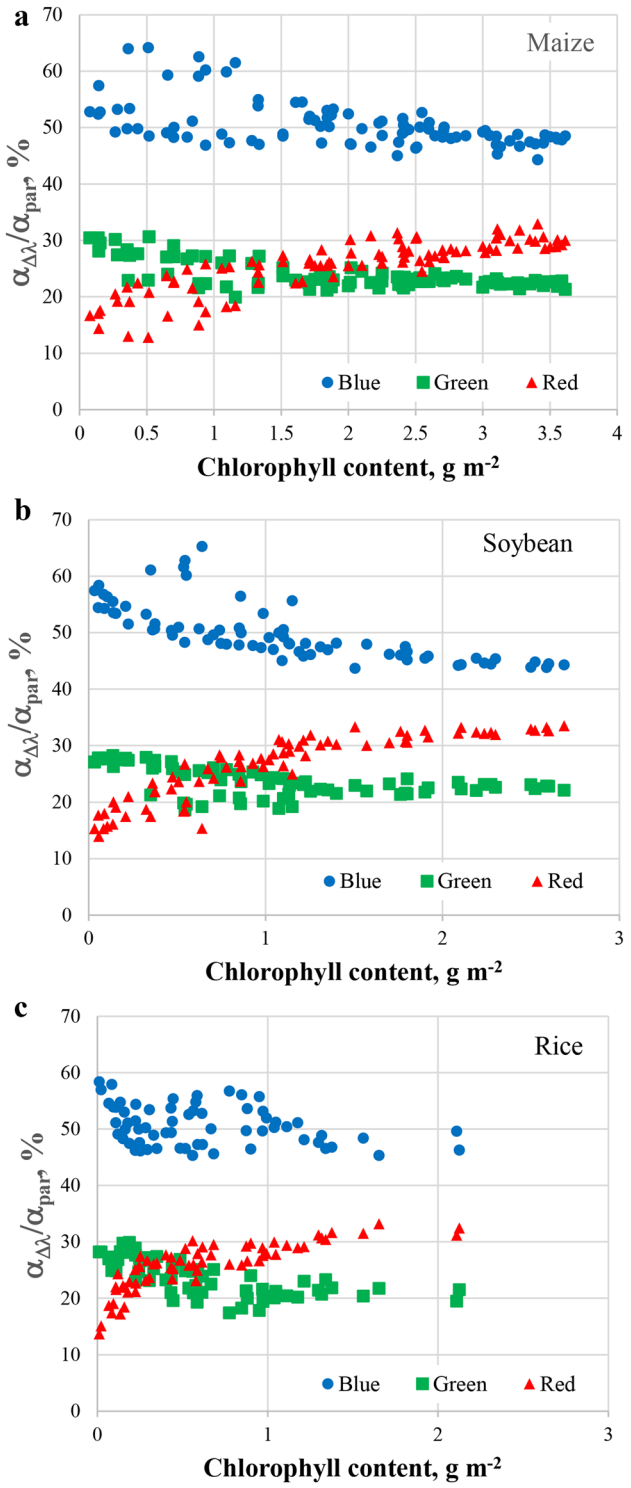

Fig. 7 Fractions of blue, green, and red light in total PAR absorption ($\alpha_{\Delta\lambda}/\alpha_{par}$) plotted vs. canopy [Chl] in **a** maize, **b** soybean, and **c** rice

The spectral change of transmittance in soybean measured at a plant half-height level (Fig. 8b) was more pronounced than in maize (Fig. 8a) and thus the green and especially the far-red fractions of the absorption coefficient

Table 3 Average quantum yield on an incident light basis and on an absorbed light basis and per cent fractions of canopy absorption coefficients, $a_{\Delta\lambda}/a_{par}$, in the blue ($\Delta\lambda = 400$–$500$ nm), green ($\Delta\lambda = 500$–600 nm), red ($\Delta\lambda = 600$–700 nm) and far-red (700–750 nm) averaged for Chl content (in g m^{-2}) across the growing season (from minimal to maximal values) and for moderate-to-high Chl content (> 1 g m^{-2}). The quantum yield values calculated per absorbed light basis are shown in bold

	[Chl] g m^{-2}	Blue	Green	Red	Far-red
Q_Y on an incident light basis		61.2	65.2	74.0	11.0
Q_Y on an absorbed light basis		**64.3**	**82.8**	**82.6**	**14.3**
$\alpha_{\Delta\lambda}/\alpha_{par}$—Maize	0–3.6	50.5	24.0	25.5	3.9
Soybean	0–2.7	51.5	25.0	23.5	2.7
Rice	0–2.1	52.5	25.0	22.5	4.8
$\alpha_{\Delta\lambda}/\alpha_{par}$—Maize	1–3.6	50.0	23.0	27.0	
Soybean	1–2.7	47.5	23.5	29.0	
Rice	1–2.1	49.0	21.0	29.0	

The quantum yield was calculated using the Supplemental Table 2 (relative basis) from (Hogewoning et al. 2012)

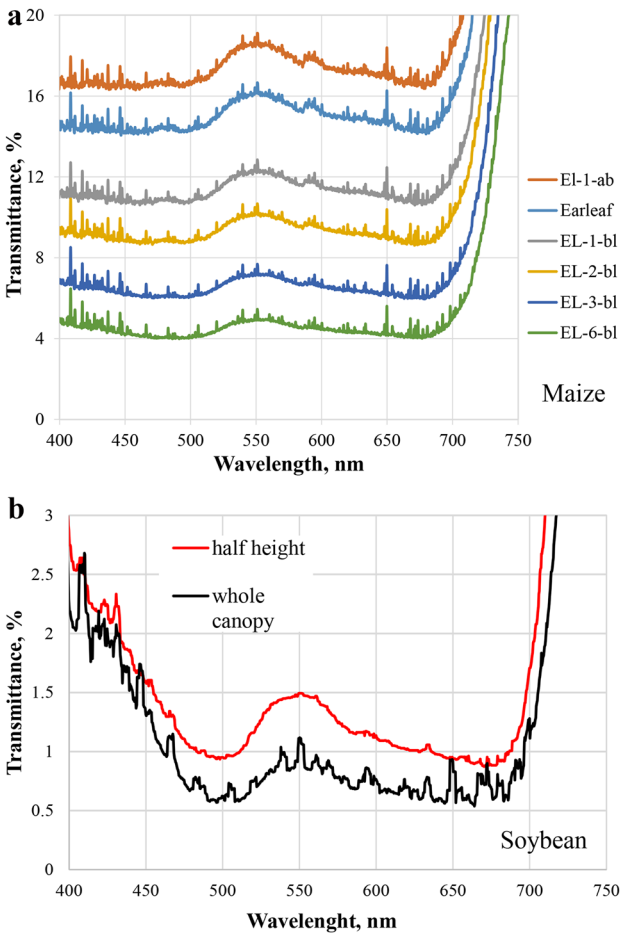

Fig. 8 **a** Transmittance of maize canopy at the level of the leaf above the ear leaf (about 1.2–1.5 m below the top of the canopy), ear leaf level, and first, second, third and sixth leaves below the ear leaf. **b** Transmittance of soybean canopy at half plant height and the whole plant

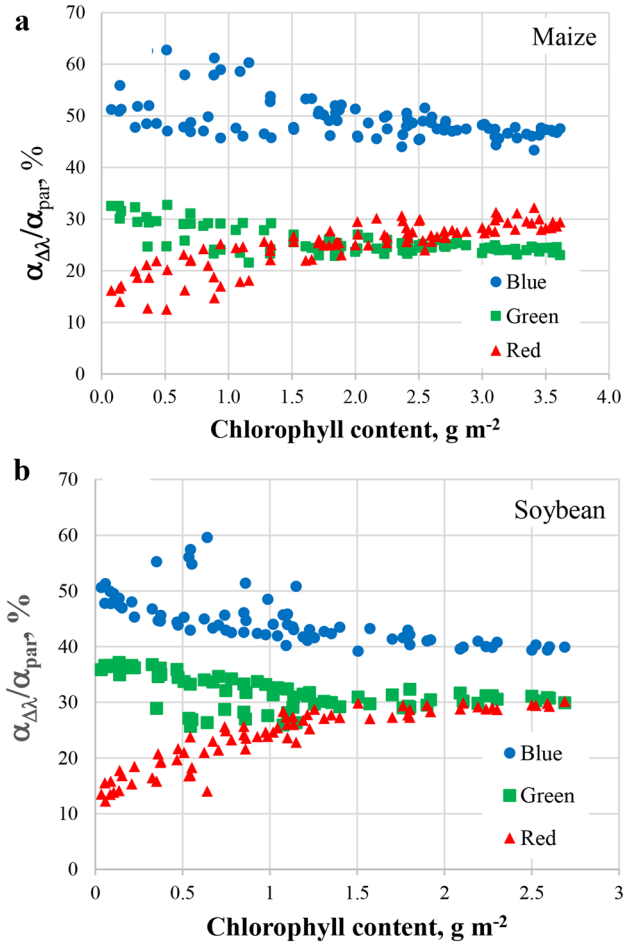

Fig. 9 **a** The fractions of PAR absorption coefficients in blue, green, and red ranges in total PAR absorption ($\alpha_{\Delta\lambda}/\alpha_{par}$) in maize canopy at the ear leaf height plotted vs. canopy Chl content. **b** The fractions of blue, green, red light in soybean canopy at a half canopy height ($\alpha_{\Delta\lambda}$) plotted vs. canopy Chl

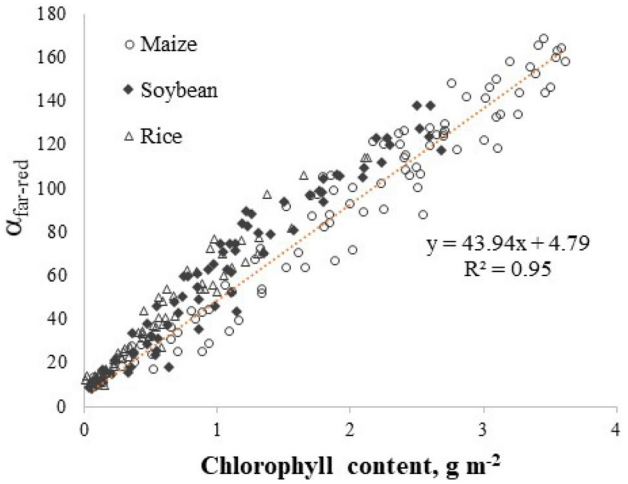

Fig. 10 Canopy absorption coefficient in the far-red spectral region, $\alpha_{far\text{-}red}$, plotted versus canopy [Chl] in three crops. $\alpha_{far\text{-}red}$ was calculated as $\alpha_{far\text{-}red} = [\rho_{NIR}/\rho_{700\text{–}750}] - 1$, where $\rho_{700\text{–}750}$ is average of canopy reflectance values in far-red region

increased significantly. For moderate-to-high [Chl] > 1 g m^{-2} the blue fraction was 41.0%, the green 31.5%, and the red 27.5% (Fig. 9b).

In the far-red range, the absorption coefficient increases substantially with an increase in total canopy [Chl] (Fig. 10), ranging between 2.7 and 4.8% of α_{par}. Notably, $\alpha_{far\text{-}red}$ is around 7% of α_{red} and about 9% of α_{green}. In the middle of the plant, the far-red absorption coefficient increased significantly reaching 3.6% of α_{par} in maize and 8.7% of α_{par} in soybean (not shown).

To understand how absorbed light in four spectral regions related to quantum yield for CO_2 fixation we compared our findings with the results of a study of quantum yield in cucumber leaves (Hogewoning et al. 2012). In Table 3 fractions of absorbed light and average relative values of quantum yields on an incident light basis and on an absorbed light basis in four spectral regions are presented (see Supplemental Table 2 in (Hogewoning et al. 2012). Average quantum yield on an incident light basis evaluated in cucumber leaves was maximal in the red; in the green it was 12% smaller than in the red. At the same time, *the quantum yields calculated on an absorbed light basis in the green and the red were equal.* If these results are relevant for the crops studied and considering that fractions of absorption coefficients in the green and the red averaged across the season are close (Table 3), it means that *in three contrasting crops CO_2 fixation driven by green light across the growing season is potentially commensurate to that driven and/or accelerated by red light.*

Furthermore, the ratio $\alpha_{far\text{-}red}/\alpha_{red}$ was 15.3% for maize, 14.5% for soybean and 21.3% for rice; the ratio of quantum yield in the far-red to that in the red, $Q_{Y(far\text{-}red)}/Q_{Y(red)}$ was 17.3%. If quantum yield calculated on the basis of absorbed light for cucumber leaves (Hogewoning et al. 2012) is applicable for the crop plants, then *the size of the far-red fraction in the light available to photosynthesis in the crop plants constitutes at least 14% of the size of light absorbed in red.*

Concluding remarks

Collectively, the findings outlined above suggest that the spectral behaviors of light capture at the leaf and plant levels display a large degree of similarity. In each spectral region (i.e., blue, green, and red), the differences between the three species in the $\alpha_{\Delta\lambda}/\alpha_{par}$ vs. [Chl] relationships were very small either at leaf (Fig. 4) or plant levels (Fig. 7) despite contrasting differences in leaf structures and canopy architectures. However, a considerable difference exists between spectral compositions of light absorbed by plants at leaf and plant

levels. The contribution of green light (500–600 nm) to the total budget of the light absorbed in PAR region is much higher at the plant level than at the leaf level; for the plant it approaches the size of the contribution of red light. This pattern was evident in the crops with disparate organization of their photosynthetic apparatuses, leaf structure, and canopy architecture.

An increase in leaf [Chl] led to a significant decline in the efficiency of light capture of this pigment; this effect was more pronounced in the bands of the Chl absorption maxima (blue and red) and much less evident in the green region where Chl absorption is relatively weak. In the blue and the red spectral regions, the incident radiation rapidly gets absorbed within the first layers of the mesophyll below the epidermis, while the inner layers of the mesophyll remain shaded. As a result, the basic assumption of independent light absorption by pigment molecules contained in the leaf is not fulfilled. Consequently, the α_λ vs. [Chl] relationship departs from linearity in these spectral regions (e.g., Gitelson et al. 2020; Naus et al. 2017). In the green region with lower absorption coefficients, light is less attenuated by the near-surface cell layers, and therefore, penetrates deeper into the leaf (Terashima et al. 2009). Thus, the α_λ vs. [Chl] relationship becomes linear and Chl efficiency is almost invariant in a wide range of its variation (Merzlyak and Gitelson 1995).

In contrast to leaves, the efficiency of Chl light absorption at the plant level remained almost invariant suggesting a uniform spectral composition of light supplied for photosynthesis throughout the growing season. This observation highlights the importance of canopy architecture for the balancing of light energy input to photosynthesis across developmental stages and different designs of photosynthetic machinery at the leaf level versus the whole-plant level (Zhang et al. 2021).

Furthermore, the results of this study have important implications for the role of green light in driving photosynthesis in dense crop stands and under volatile illumination conditions. It is debated that the green gap in the absorption spectrum of plants is merely a consequence of chemical and photophysical properties of chlorophylls, the ubiquitous primary photosynthetic pigments of terrestrial plants. Results presented above suggest that the energy supply by green light can be commensurate to that of red light. At the same time, the quantum yield of green light, calculated on the basis of absorbed light, is comparable with that of red light, and greater than that of blue light (e.g., (Hogewoning et al. 2012)). The important role of green light is conclusively supported by the estimations of the contribution of radiation in the green range (500–600 nm) to the total absorbed energy budget as discussed above. It is important to note that action spectra of leaf photosynthesis have been measured with weak monochromatic light (Oguchi et al. 2011; Inada 1976) while absorption properties of crops have been measured in strong light where the quantum yield of green light exceeds those in blue and red ranges (Wu et al. 2019). Terashima et al. (2009) found that differential quantum yield of green light in a sunflower leaf in moderate to strong white light was greater than in red light. Thus, fractions of absorbed radiation and quantum yield of photosynthesis may be even closer than presented in Table 3.

Green light has a quantum efficiency higher or equivalent to that of blue light, and it is transmitted through the leaf and to underlying leaves where it can actively drive photosynthesis. The significant decrease of transmittance in the green region with an increasing number of leaf layers (Fig. 8) clearly demonstrates the utilization of green light deeper in the canopy. This can be especially important in the case of plants encountering very high fluxes of solar radiation when leaves in the upper layers of the canopy become rapidly inhibited by the radiation in the red and blue parts of the spectrum (Oguchi et al. 2021). In such situations, most of the carbon fixation is done by the shaded leaves lower in the canopy powered predominantly by green light. This might be the rationale for large metabolic investments of many plant species, including the studied crop plants, in growing dense canopies and retaining green leaves deep within the canopy.

The canopy absorption coefficient in the far-red region is not negligible: $\alpha_{\text{far-red}}$ was around 7–10% of the absorption coefficient fractions in the green and red regions. Still, the role of far-red light is underexplored. The results of our analysis of the light energy budget show that a sizeable portion of light available deep in the canopy (as in lower leaf layers) consists of radiation in this range. To date, a large body of evidence has been accumulated supporting the feasibility of using this spectral range as an energy source, mostly to ensure proper unloading of the chloroplast electron transport chain and thus avoid photooxidative damage (Kono et al. 2020; Allakhverdiev 2020; Wolf and Blankenship 2019). The combination of a considerable proportion of the energy in this spectral range and the capability of plants to absorb radiation in this range further supports an important role of far-red radiation in supplementing the energy budget of plants and maintaining their acclimation to high light fluxes (Wu et al. 2021).

Finally, it is important to underline that the role of green light in photosynthesis was demonstrated here in simple experiments in natural conditions (e.g., crops in the field) as absorption properties were retrieved from remotely measured reflectance. This approach allowed the quantification of different fractions of light absorbed by vegetation and highlighted the role of green light in photosynthesis. An important extension of this idea is the experimental support for the role of radiation in the far-red region of the spectrum as an energy source for shaded leaves located deep within plant canopies. While this study

is more proof-of-concept than finalized product, the results suggest the potential for using leaf and plant absorption coefficient retrieved from reflectance to quantify potential photosynthesis in each spectral range.

Acknowledgements A.S. acknowledges the support from Shared Access Center of Derzhavin Tambov State University user facilities.

Funding The support and use of facilities and equipment provided by the Center for Advanced Land Management Information Technologies (CALMIT), the School of Natural Resources, and the Carbon Sequestration Program, all at the University of Nebraska-Lincoln, are greatly appreciated. This research was partially supported by the Nebraska Agricultural Experiment Station with funding from the Hatch Act (Accession Number 1002649) through the USDA National Institute of Food and Agriculture. Funding for AmeriFlux data resources was provided by the U.S. Department of Energy's Office of Science. A.S. acknowledges the support of Russian Foundation for Basic Research (Grant Number 19-016-00016).

Data availability The raw data are available from the authors on reasonable request.

Declarations

Conflict of interest The authors do not have any conflict of interest.

Appendix

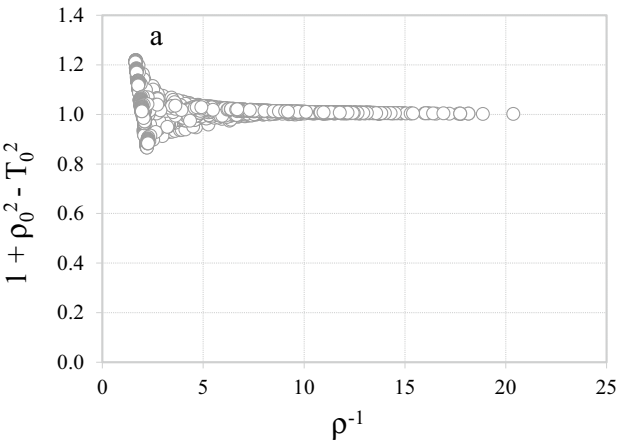

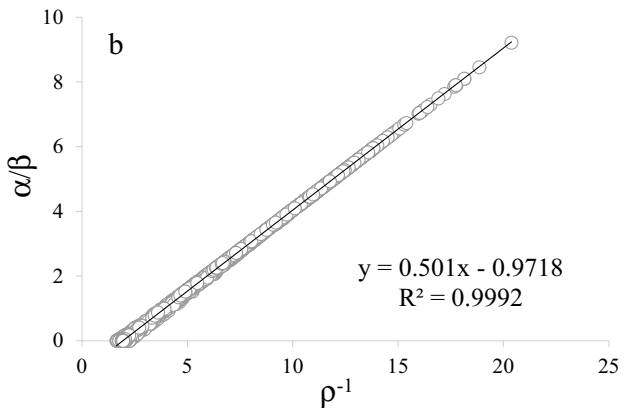

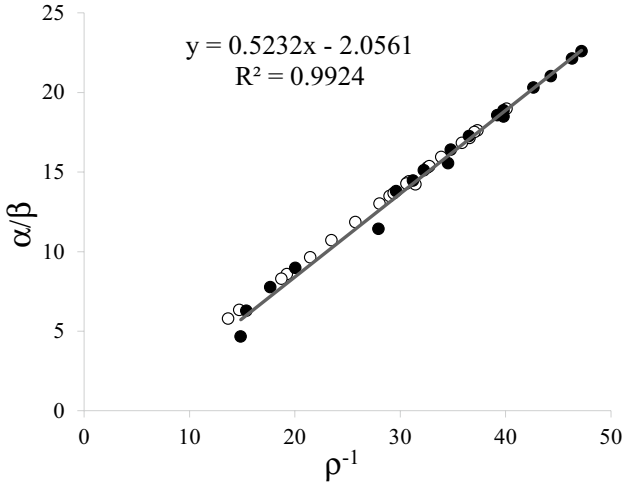

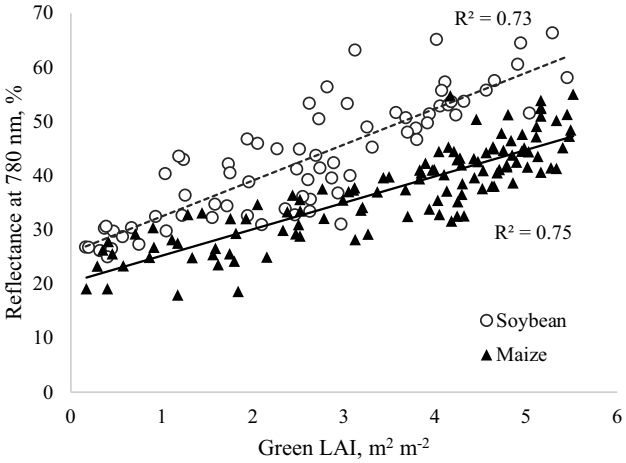

References

Allakhverdiev SI (2020) Optimising photosynthesis for environmental fitness. Funct Plant Biol 47(11):iii–vii. https://doi.org/10.1071/FPv47n11_FO

Ciganda V, Gitelson A, Schepers J (2009) Non-destructive determination of maize leaf and canopy chlorophyll content. J Plant Physiol 166(2):157–167

Cui M, Vogelmann T, Smith W (1991) Chlorophyll and light gradients in sun and shade leaves of *Spinacia oleracea*. Plant Cell Environ 14(5):493–500

Feret J-B, François C, Asner GP, Gitelson AA, Martin RE, Bidel LPR, Ustin SL, le Maire G, Jacquemoud S (2008) PROSPECT-4 and 5: advances in the leaf optical properties model separating photosynthetic pigments. Remote Sens Environ 112:3030–3043. https://doi.org/10.1016/j.rse.2008.02.012

Féret J-B, Gitelson A, Noble S, Jacquemoud S (2017) PROSPECT-D: towards modeling leaf optical properties through a complete lifecycle. Remote Sens Environ 193:204–215

Gates DM (1980) Solar radiation. In: Biophysical ecology. Springer, New York, pp 96–147

Gitelson AA, Gritz Y, Merzlyak MN (2003) Relationships between leaf chlorophyll content and spectral reflectance and algorithms for non-destructive chlorophyll assessment in higher plant leaves. J Plant Physiol 160(3):271–282

Gitelson AA, Viña A, Ciganda V, Rundquist DC, Arkebauer TJ (2005) Remote estimation of canopy chlorophyll content in crops. Geophys Res Lett. https://doi.org/10.1029/2005GL022688

Gitelson AA, Viña A, Verma SB, Rundquist DC, Arkebauer TJ, Keydan G, Leavitt B, Ciganda V, Burba GG, Suyker AE (2006) Relationship between gross primary production and chlorophyll content in crops: implications for the synoptic monitoring of vegetation productivity. J Geophys Res Atmos. https://doi.org/10.1029/2005JD006017

Gitelson AA, Viña A, Masek JG, Verma SB, Suyker AE (2008) Synoptic monitoring of gross primary productivity of maize using Landsat data. IEEE Geosci Remote Sens Lett 5(2):133–137

Gitelson AA, Peng Y, Viña A, Arkebauer T, Schepers JS (2016) Efficiency of chlorophyll in gross primary productivity: a proof of concept and application in crops. J Plant Physiol 201:101–110

Gitelson AA, Arkebauer TJ, Suyker AE (2018) Convergence of daily light use efficiency in irrigated and rainfed C3 and C4 crops. Remote Sens Environ 217:30–37

Gitelson A, Viña A, Solovchenko A, Arkebauer T, Inoue Y (2019) Derivation of canopy light absorption coefficient from reflectance spectra. Remote Sens Environ 231:111276

Gitelson A, Solovchenko A, Viña A (2020) Foliar absorption coefficient derived from reflectance spectra: a gauge of the efficiency of in situ light-capture by different pigment groups. J Plant Physiol 254:153277

Gitelson A, Arkebauer T, Viña A, Skakun S, Inoue Y (2021) Evaluating plant photosynthetic traits via absorption coefficient in the photosynthetically active radiation region. Remote Sens Environ. https://doi.org/10.1016/j.rse.2021.112401

Hanan NP, Burba G, Verma SB, Berry JA, Suyker A, Walter-Shea EA (2002) Inversion of net ecosystem CO_2 flux measurements for estimation of canopy PAR absorption. Glob Change Biol 8(6):563–574

Hogewoning SW, Wientjes E, Douwstra P, Trouwborst G, van Ieperen W, Croce R, Harbinson J (2012) Photosynthetic quantum yield dynamics: from photosystems to leaves. Plant Cell 24(5):1921–1935. https://doi.org/10.1105/tpc.112.097972

Inada K (1976) Action spectra for photosynthesis in higher plants. Plant Cell Physiol 17(2):355–365

Inoue Y, Guérif M, Baret F, Skidmore A, Gitelson A, Schlerf M, Darvishzadeh R, Olioso A (2016) Simple and robust methods for remote sensing of canopy chlorophyll content: a comparative analysis of hyperspectral data for different types of vegetation. Plant Cell Environ 39(12):2609–2623

Kono M, Kawaguchi H, Mizusawa N, Yamori W, Suzuki Y, Terashima I (2020) Far-red light accelerates photosynthesis in the low-light phases of fluctuating light. Plant Cell Physiol 61(1):192–202. https://doi.org/10.1093/pcp/pcz191

Kortum G (1969) Reflectance spectroscopy. In: Principles, methods, applications. Springler-Verlag Inc., New York, NY

Kubelka P, Munk F (1931) Ein Beitrag Zur Optik Der Farbanstriche. Z Tech Phys 12:593–601

Kume A (2017) Importance of the green color, absorption gradient, and spectral absorption of chloroplasts for the radiative energy balance of leaves. J Plant Res 130(3):501–514

Laisk A, Oja V, Eichelmann H, Dall'Osto L (2014) Action spectra of photosystems II and I and quantum yield of photosynthesis in leaves in State 1. Biochem Biophys Acta 2:315–325

Lichtenthaler H (1983) Differences in chlorophyll levels, fluorescence and photosynthetic activity of leaves from high-light and low-light seedlings. In: Photosynthesis and plant productivity: joint meeting of OECD and Studienzentrum Weikersheim, Ettlingen Castle (Germany), October 11–14, 1981/editor: H. Metzner. Wissenschaftliche Verlagsgesellschaft, Stuttgart

Marosvölgyi M, van Gorkom H (2002) Cost and color of photosynthesis. Photosynth Res 103(2):105–109

McCree KJ (1971) The action spectrum, absorptance and quantum yield of photosynthesis in crop plants. Agric Meteorol 9:191–216

Merzlyak MN, Gitelson A (1995) Why and what for the leaves are yellow in autumn? on the interpretation of optical spectra of senescing leaves (acerplatanoides l.). J Plant Physiol 145:315–320

Merzlyak MN, Chivkunova OB, Melo TB, Naqvi KR (2002) Does a leaf absorb radiation in the near infrared (780–900 nm) region? A new approach to quantifying optical reflection, absorption and transmission of leaves. Photosynth Res 72(3):263–270. https://doi.org/10.1023/A:1019823303951

Merzlyak MN, Melø T, Naqvi KR (2004) Estimation of leaf transmittance in the near infrared region through reflectance measurements. J Photochem Photobiol B 74(2–3):145–150

Naus J, Lazar D, Barankova B, Arnostova B (2017) On the source of non-linear light absorbance in photosynthetic samples. Photosynth Res. https://doi.org/10.1007/s11120-017-0468-6

Nishio JN, Sun J, Vogelmann TC (1993) Carbon fixation gradients across spinach leaves do not follow internal light gradients. Plant Cell 5(8):953–961

Oguchi R, Douwstra P, Fujita T, Chow WS, Terashima I (2011) Intra-leaf gradients of photoinhibition induced by different color lights: implications for the dual mechanisms of photoinhibition and for the application of conventional chlorophyll fluorometers. New Phytol 191(1):146–159. https://doi.org/10.1111/j.1469-8137.2011.03669.x

Oguchi R, Terashima I, Chow WS (2021) The effect of different spectral light quality on the photoinhibition of photosystem I in intact leaves. Photosynth Res. https://doi.org/10.1007/s11120-020-00805-z

Paradiso R, Meinen E, Snel JF, De Visser P, Van Ieperen W, Hogewoning SW, Marcelis LF (2011) Spectral dependence of photosynthesis and light absorptance in single leaves and canopy in rose. Sci Hortic 127(4):548–554

Peng Y, Gitelson AA, Keydan G, Rundquist DC, Moses W (2011) Remote estimation of gross primary production in maize and support for a new paradigm based on total crop chlorophyll content. Remote Sens Environ 115(4):978–989

Peng Y, Nguy-Robertson A, Arkebauer T, Gitelson AA (2017) Assessment of canopy chlorophyll content retrieval in maize and soybean: implications of hysteresis on the development of generic algorithms. Remote Sens 9(3):226

Pettai H, Oja V, Freiberg A, Laisk A (2005) Photosynthetic activity of far-red light in green plants. Biochem Biophys Acta 1708(3):311–321

Rundquist D, Perk R, Leavitt B, Keydan G, Gitelson A (2004) Collecting spectral data over cropland vegetation using machine-positioning versus hand-positioning of the sensor. Comput Electron Agric 43(2):173–178

Sun J, Nishio J, Vogelmann T (1998) Green light drives CO_2 fixation deep within leaves. Plant Cell Physiol 39(10):1020–1026

Terashima I, Saeki T (1985) A new model for leaf photosynthesis incorporating the gradients of light environment and of photosynthetic properties of chloroplasts within a leaf. Ann Bot 56(4):489–499

Terashima I, Fujita T, Inoue T, Chow W, Oguchi R (2009) Green light drives leaf photosynthesis more efficiently than red light in strong white light: revisiting the enigmatic question of why leaves are green. Plant Cell Physiol 50(4):684–697

Terashima I, Hiroki O, Takashi F, Riichi O (2016) Light environment within a leaf. II. Progress in the past one-third century. J Plant Res 129(3):353–363. https://doi.org/10.1007/s10265-016-0808-1

Verma SB, Dobermann A, Cassman KG, Walters DT, Knops JM, Arkebauer TJ, Suyker AE, Burba GG, Amos B, Yang H (2005) Annual carbon dioxide exchange in irrigated and rainfed maize-based agroecosystems. Agric For Meteorol 131(1–2):77–96

Viña A (2004) Remote estimation of leaf area index and biomass in corn and soybean. PhD Dissertation—University of Nebraska-Lincoln

Viña A, Gitelson AA, Nguy-Robertson AL, Peng Y (2011) Comparison of different vegetation indices for the remote assessment of green leaf area index of crops. Remote Sens Environ 115(12):3468–3478

Vogelmann T (1993) Plant tissue optics. Annu Rev Plant Biol 44(1):231–251

Wendlandt WWM, Hecht HG (1966) Reflectance spectroscopy. Wiley, New York, NY

Wolf BM, Blankenship RE (2019) Far-red light acclimation in diverse oxygenic photosynthetic organisms. Photosynth Res 142(3):349–359. https://doi.org/10.1007/s11120-019-00653-6

Wu BS, Rufyikiri AS, Orsat V, Lefsrud MG (2019) Re-interpreting the photosynthetically action radiation (PAR) curve in plants. Plant Sci 289:110272. https://doi.org/10.1016/j.plantsci.2019.110272

Wu H-Y, Liu L-A, Shi L, Zhang W-F, Jiang C-D (2021) Photosynthetic acclimation during low-light-induced leaf senescence in post-anthesis maize plants. Photosynth Res. https://doi.org/10.1007/s11120-021-00851-1

Zhang N, Evers JB, Anten NPR, Marcelis LFM (2021) Turning plant interactions upside down: light signals from below matter. Plant Cell Environ 44(4):1111–1118. https://doi.org/10.1111/pce.13886

Zhen S, Haidekker M, van Iersel MW (2019) Far-red light enhances photochemical efficiency in a wavelength-dependent manner. Physiol Plant 167(1):21–33